



Airborne measurements for investigating offshore wind farm wakes and modifications of sea state - benefits and limitations

Astrid Lampert¹, Beatriz Cañadillas¹, Thomas Rausch¹, Lea Schmitt¹, Bughsin' Djath², Johannes Schulz-Stellenfleth², Andreas Platis³, Kjell zum Berge³, Ines Schaefer³, Jens Bange³, Thomas Neumann⁴, Martin Dörenkämper⁵, Bernhard Stoevesandt⁵, Julia Gottschall^{5,6}, Lukas Vollmer⁵, Stefan Emeis⁷, Mares Barekzai⁷, Simon Siedersleben⁷, Martin Kühn^{8,9}, Gerald Steinfeld^{8,9}, Detlev Heinemann^{8,9}, Joachim Peinke^{8,9}, Hendrik Heißelmann^{8,9}, Jörge Schneemann^{8,9}, Gabriele Centurelli^{8,9}, Philipp Waldmann¹, and Konrad Bärfuss¹

¹TU Braunschweig, Institute of Flight Guidance, Hermann-Blenk-Str. 27, 38108 Braunschweig, Germany

²Helmholtz-Zentrum Hereon, Institute of Coastal Systems - Analysis and Modeling, Max-Planck-Str. 1, 21502 Geesthacht, Germany

³Environmental Physics, Eberhard Karls University of Tübingen, Schnarrenbergstr. 94-96, 72076 Tübingen, Germany

⁴FGW e.V. – Fördergesellschaft Windenergie und andere Dezentrale Energien, Oranienburger Str. 45, 10117 Berlin, Germany

⁵Fraunhofer IWES, Küppersweg 70, 26129 Oldenburg, Germany

⁶Faculty of Geosciences, University of Bremen, 28359 Bremen, Germany

⁷Karlsruhe Institute of Technology (KIT), Institute of Meteorology and Climate Research, Kreuzeckbahnstr. 19, 82467 Garmisch-Partenkirchen, Germany

⁸Carl von Ossietzky Universität Oldenburg, School of Mathematics and Science, Institute of Physics, Germany

⁹ForWind - Center for Wind Energy Research, Küppersweg 70, 26129 Oldenburg, Germany

Correspondence: Astrid Lampert (Astrid.Lampert@tu-braunschweig.de)

Abstract. In the framework of the two large wind energy research projects WIPAFF and X-Wakes, crewed airborne measurements have been performed in and around wind farm clusters of the German Bight to investigate offshore wind farm wakes and associated sea-state modifications. These flights offer high spatial flexibility. Routes can be adapted in real time to wind direction, stability, wake extent, and features of interest, providing complementary coverage to fixed ground-based instruments and remote sensing systems. Aircraft observations achieve high vertical resolution in the order of several centimetres and allow simultaneous measurements of wind speed, turbulence, thermodynamic variables, air-sea fluxes, and sea surface characteristics. This enables a detailed description of wake structure, wake recovery, and the influence of atmospheric stability, as well as the interaction of multiple wakes across scales of tens to hundreds of kilometres. Airborne measurements also provide a direct link between atmospheric changes and sea-surface modifications, such as altered roughness or wave patterns, and supply valuable data for evaluating simulations and improving parameterizations used in wind farm modelling. When combined with satellite remote sensing, they help bridge the gap between high-resolution local observations and large-area coverage. A central limitation of aircraft campaigns is their restricted temporal coverage. Flights are episodic and sample evolving atmospheric conditions over finite time periods, which complicates the comparison with satellite snapshots and limits the ability to derive long-term statistics. As small wind farm effects that are in the order of the natural variability of the background flow are easily masked by natural variability in the marine boundary layer, effects such as global blockage are difficult to isolate



using aircraft data alone. Overall, aircraft-based observations offer unique strengths when integrated with other measurement systems and modelling tools, despite inherent temporal constraints. This article summarizes which effects benefit from the analysis of airborne data sets, and shows examples where they helped to improve the understanding of the interaction of wind farms, atmosphere and sea state significantly.

20 1 Introduction

The transformation of energy towards renewable resources requires the worldwide installation of large capacities of wind power. In particular, offshore wind farm clusters play a key role in the increase of the share of renewables, as offshore sites typically offer more reliable and stronger wind conditions than onshore locations (Veers et al., 2019). The globally installed offshore wind capacity is expected to increase from 75.2 GW (as of 2024) to 380 GW by 2030, and to 2,000 GW by 2050. In 25 Germany, an installation of a total capacity of 30 GW is planned until 2030, and even 70 GW until 2045 (Global Offshore Wind Report, 2025).

Nowadays it is common knowledge that offshore wind farms are associated with wind farm wakes, which are an area of reduced wind speed and increased turbulence downwind (e.g., Platis et al., 2018; Schneemann et al., 2020), and airborne measurements provided key data to quantify wake extent and wind speed recovery (Platis et al., 2020).

30 In the future, with the strong increase in offshore installations of wind capacities, an increasing area will be influenced by wind farm wakes (Pryor and Barthelmie, 2021; Akhtar et al., 2021; Bodini et al., 2021). Especially wake impacts on downstream farms have become increasingly important in the overall planning of offshore farms in recent years (Ouro et al., 2025). The installation and operation of these large offshore wind farms have environmental and technological consequences (Bailey et al., 2014; Windt et al., 2024), including a different visual appearance (Ladenburg, 2009), which is, however, avoided for 35 the German Bight by wind farm locations far from the coast. Large wind farms can modify the atmospheric boundary layer, cloudiness and precipitation (Akhtar et al., 2022). For the additional implementation of offshore wind farms, the overall mutual impacts of and on the existing wind farms and their wakes have to be taken into account (Christiansen et al., 2023). This refers to reduced available wind resource as well as increased downstream turbulence, which has an impact on fatigue loadings within wind farms (Sathe et al., 2012; Lee et al., 2013; Vera-Tudela and Kühn, 2017), but only very limited impact for far 40 downstream cluster wakes (Anantharaman et al., 2025). Further, the impact on sea state (Bärfuss et al., 2021; Schmitt et al., 2025), ocean stratification (Lian et al., 2022; Christiansen et al., 2022) and ocean circulation (Broström, 2008) are supposed to increase, with secondary effects for the ecosystem (Daewel et al., 2022). As the electrical grid and feed-in planning relies on an increasing share of the highly flexible resource of wind power (Drew et al. , 2015), it is of crucial importance to be able to predict the power output with high reliability on the time scale of days and hours. Also for investment, the knowledge of the 45 wind resource is essential (Mora et al., 2019). Further, with increasing impact of wakes on neighbouring wind farms, resulting in reduced energy output (Lundquist et al., 2019), international planning gains importance (Finserås et al., 2024). Therefore the phenomenon of wind farm wakes is of large importance. An enhanced understanding of wake characterization is required to develop suitable parametrizations for wind farm models of different complexity, from fast engineering models (Bastankhah



and Porté-Agel, 2014; Nygaard et al., 2020) to mesoscale weather models (Fitch et al., 2012; Vollmer et al., 2024). In contrast, 50 large eddy simulations, LES (Wu and Porté-Agel, 2011; Dörenkämper et al., 2015), fully resolve turbines, assuming actuator disks to be a sufficiently good representation. At the same time, LES cannot be used for resource assessment due to the large computational costs. As mentioned in several overview articles, the lack of offshore data characterizing the marine atmospheric boundary layer is a major drawback for improving understanding and simulations (Veers et al., 2019; Shaw et al., 2022).

The motivation to perform airborne measurements to characterize the properties of offshore wind farm wakes was motivated 55 in 2012 by radar satellite images, where a modification of the water surface downstream of wind farm areas was evident (Christiansen and Hasager, 2005), and first simulations suggesting a much higher wind speed deficit and long-reaching wakes under stable atmospheric conditions (Fitch et al., 2012; Abkar et al., 2016). The first project for airborne in-situ measurements in the wake of offshore wind farms, WIPAFF, was finally granted in 2015 (Emeis et al., 2016). This first project proved the existence of far-reaching wind farm wakes extending several 10 km under stable atmospheric conditions, and provided a first 60 idea of the impact of wakes on the sea surface. Another proposal was initiated in 2017, and finally the project called X-Wakes was funded with an extended consortium in 2019.

The article presents progress in the field of offshore wind farm wake research based on measurements with manned aircraft. To the authors' knowledge, these are so far the only airborne observations worldwide with the purpose to study the wakes of 65 entire wind farms. It summarizes results that are already published, and adds new aspects, which have not yet been published so far. It is structured as follows: Sect. 2 introduces the methodology of airborne in-situ measurements of offshore wind farm wakes. Sect. 3 presents an overview of several phenomena associated with offshore wind farm wakes that were investigated with airborne measurements: Sect. 3.1 provides the improvement of wake characterization by airborne observations. Sect. 3.2 demonstrates the interaction of wakes of different wind farms. Sect. 3.3 shows the modification of latent heat fluxes in wakes, which may be responsible for local cloud formation at wind farms. Sect. 3.4 provides an overview of coastal effects, which 70 is the modification of the wind field across the coast line. Sect. 3.5 presents airborne data as used for model validation. Sect. 3.6 demonstrates the link of wind farm wakes to modified sea surface properties. Sect. 3.7 illustrates the limits of airborne measurements, which is the observation of small effects due to the limited observation time and constraints in flight patterns close to wind farms, with the example of the global blockage effect. Finally, Sect. 4 summarizes the results in the conclusions.

2 Methodology of airborne in-situ wake measurements

75 The airborne offshore wind farm wake measurements were mainly performed with the research aircraft Dornier 128 with call sign D-IBUF of TU Braunschweig (Corsmeier et al., 2001; Lampert et al., 2020), and in addition several flights were done in parallel with the research aircraft Cessna F406 with call sign D-ILAB of TU Braunschweig (Lampert et al., 2024). The meteorological instrumentation for measuring the high resolution (100 Hz) wind vector, temperature and humidity is installed in the nose boom. The typical air speed is 70 m s^{-1} . Additional instrumentation for measuring surface temperature and sea 80 state is installed in the aircraft cabin.

The measurements for investigating wind farm wakes were performed at hub height crossing the wind farm wake perpendicular



to the wind direction at different downstream distances. In addition, vertical profiles from very low altitudes (15 m) to the free troposphere (1 km) were integrated in the flight pattern regularly to determine atmospheric stability, vertical wind profiles, and the temporal and spatial variability of the wind field. Each horizontal flight leg across the wake typically had a distance
85 of 40 km in order to capture also the undisturbed flow to both sides, and took around 10 min. Also the upstream conditions were probed. For investigating wake interactions, flights across wake areas were done between and downstream of different wind farms. The overall duration of one flight, including the ferry from the airport with jigsaw patterns of vertical profiles to investigate the spatial development of the ABL, then the pattern to sample the wake, including the vertical profiles in between the legs, and the ferry back, was around 4 h. Other flight patterns were dedicated to changes of meteorological parameters
90 above the wind farms, to the global blockage effect with upstream measurements, and to modifications of the atmospheric boundary layer induced by the influence of the coast. Detailed explanations of the aircraft, the sensors and the different flight patterns are provided in Lampert et al. (2020) and Lampert et al. (2024).

In addition to continuous measurements at fixed locations, airborne measurements provide the opportunity to determine the spatial variability and a complementary data set for intensive observation periods. This allows to study the representativeness of
95 continuous profile measurements, like at the meteorological masts FINO1, e.g. Wagner et al. (2019); Spangeli et al. (2023), and FINO3, e.g. Peña et al. (2015); Olsen et al. (2022) for the German Bight (Platis et al., 2021). Further, lidar profile measurements at one location can be embedded in the context of spatial variability of the wind field by airborne observations (Cañadillas et al., 2022). Airborne measurements can also be used to characterize the sensitivity of stability definitions on the height interval of local measurements, e.g., air temperature at only two heights compared to a high resolution aircraft profile (Platis et al.,
100 2021). The analysis of airborne measurements has to take into account the synoptic spatial and temporal variability of the wind field. Stationary conditions cannot be assumed over the 4 h time period of a research flight. Therefore, it turned out to be not possible to use the upstream wind field as a reference for the downstream modifications, as planned originally. Instead, the wind speed in the wake area was compared to the wind speed in the undisturbed area next to the wind farm wake area for each of the flight legs (Cañadillas et al., 2020). Spatial gradients of the wind field across the wake area were frequently present as
105 well (Platis et al., 2018).

3 Airborne observations of offshore wind farm wakes and associated phenomena

In the following, different aspects of offshore wind farm wakes are considered from the perspective of airborne measurements, as published in the Data Publisher for Earth & Environmental Science PANGAEA (Rausch et al., 2023a). As the wind speed data in the published datasets show a small intriguing cross correlation regarding the wind impact angle on the flight path
110 – likely caused by pressure transducers with temperature / temperature gradient dependency outside their specification – the wind speed data were corrected by the assumption of a constant sideslip angle error for the analyses in Sect. 3.1 and Sect. 3.2, with subsequent median filtering over a time window of 30 s. The wind speed correction has been done by deriving the wind speed error from an already simplified wind derivation equation (see e.g. Bärfuss et al. (2023), Equation A16) in addition to small angle approximations, which alter the wind speed depending on whether wind is faced star- or backboards of the aircraft.



115 Assuming an absolute angular error of 0.3° on the angle of sideslip and a measurement speed of 65 m s^{-1} , the wind error is $\pm 0.35 \text{ s}^{-1}$ on flight legs perpendicular to the prevailing wind direction.

3.1 Wind farm wake characterization

The characterization of wind farm wakes was done by performing meander patterns, i.e., individual flight tracks, called legs, oriented perpendicular to the prevailing wind direction. Typically, in the framework of the campaigns conducted in the projects 120 WIPAFF and X-Wakes, the transects through the wake area were spaced with a horizontal distance of 10 km. The closest flight leg was at a distance of 500 m downstream of the wind farm due to flight permissions. For neutral and unstable conditions, the distance between the flight legs was reduced. Like this, the horizontal extent and the wind speed recovery of wind farm wakes were quantified. Wakes extend downstream to several km under neutral conditions (Cañadillas et al., 2020) and can be observed 125 at least several 10 km downstream under stable atmospheric conditions (Platis et al., 2018). The recovery of the wind speed can be approximated by an exponential function, with a typical recovery to 95% of the undisturbed wind speed after a downstream distance of around 55 km for stable and 20 km for unstable conditions (Cañadillas et al., 2020), with high variability (Foreman et al., 2025). This recovery, in particular for stable conditions, is significantly slower than usually assumed in industry models 130 (Cañadillas et al., 2020; Platis et al., 2020) but in the order of magnitude predicted by simple analytical stability-dependent wind farm models such as EFFWAKE (Emeis, 2010, 2022). The wake length (Platis et al., 2020) and also the initial wind speed deficit directly downwind of the wind farms (Platis et al., 2021) strongly depend on atmospheric stability, but also other 135 parameters, like wind farm geometry and density seem to have a major influence. Downstream of wind farms, vertical mixing is enhanced at the altitude range of the rotor blades. This vertical mixing can result in micrometeorological changes, either warming or cooling of the air at hub height, and either drying or moistening of the downstream atmosphere, which depends on the altitude of the temperature inversion and the moisture distribution with height (Siedersleben et al., 2018b). The airborne measurements show that directly above the wind farms, turbulence is strongly increased (Siedersleben et al., 2020).

As an illustration, Fig. 1 shows wind speed at 10 m height derived from a synthetic aperture radar (SAR) image. The radar data were obtained on 11 September 2021 at 17:17 UTC, and the 10-m wind speed with a horizontal resolution of 300 m was derived from the normalized radar cross section (NRCS) using a C-band geophysical model function CMOD5N (Hersbach et al., 2007; Verhoef et al., 2017; Djath et al., 2018). Fig. 2 displays an almost temporally overlapping measurement flight carried 140 out in the same area between 12:51 and 17:13 UTC. The SAR snapshot provides a quasi-synoptic view of the near-surface wind field at the end of the flight period, while the aircraft sampled the same flow along several transects at hub height and in vertical profiles. Downstream of the wind-farm cluster N4, both observations capture a decrease of the wind speed for the individual wind farms Amrumbank West, Nordsee Ost and Meerwind Süd-Ost (from north to south), and a speed-up in the so-called "Kaskasi gap" between Amrumbank West and Nordsee Ost, where the wind farm Kaskasi was built after the flights were 145 conducted. For a more detailed comparison, Fig. 3 shows the wind speed measured along three horizontal transects (T6, T7 and T8). Satellite-based estimates typically derive the wind speed at hub height in several steps indirectly from the height of the capillary waves at the surface that are an indicator for the winds and roughness at the surface. From those, the 10 m wind speed is derived first. Then the SAR-derived 10-m wind speed was extrapolated to hub height using stability information obtained

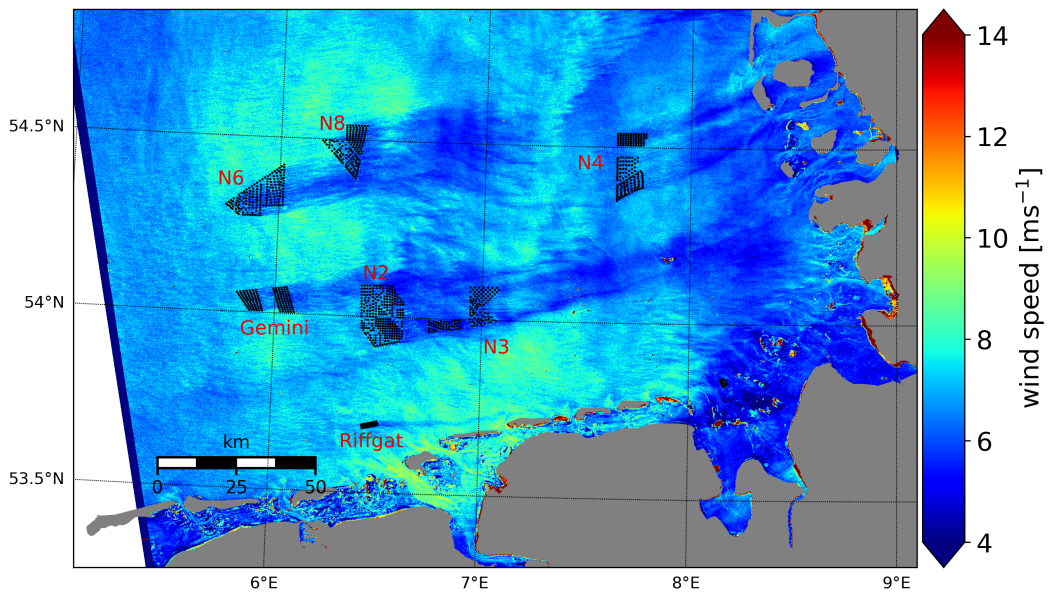


Figure 1. Derived 10-m wind speed from Sentinel-1A SAR (Contains modified Copernicus Sentinel data [2021]) data acquired on 11 September 2021 at 17:17 UTC. Black dots represent wind turbines; names of wind farms and clusters are labelled in red. The wind direction is from West. Powered by Esri.

from the airborne profiles. Airborne in-situ measurements along these transects show substantial small-scale variability and 150 enhanced turbulence, whereas the collocated SAR-derived hub-height winds provide smoother fields because of the finite radar footprint and the averaging applied in the retrieval (Djath et al., 2018). Despite the high-frequency fluctuations observed in the airborne data, the SAR-derived wind speed closely follows the mean airborne signal for all transects. Small discrepancies are visible, particularly in regions of enhanced turbulence (e.g. at distances of around 0.5–1.5 km for the transects at 16:49 UTC and 17:04 UTC), but the overall agreement is high in both magnitude and spatial patterns. The joint analysis highlights 155 the complementarity between airborne and satellite observations in offshore wind-farm wake studies. Aircraft measurements provide an independent reference at hub height and resolve turbulence and vertical shear on scales that cannot be captured by SAR, thereby supplying essential context for interpreting SAR-derived wake signatures. At the same time, SAR offers an instantaneous, spatially extensive view of the near-surface wind field that cannot be achieved by aircraft alone. Together, these platforms show that SAR-derived wind speed can reliably reproduce the horizontal wind field at hub height when combined 160 with appropriate stability information, and can therefore serve as a consistent complement to airborne measurements.

Overall, compared to other wake measurement methods, airborne measurements offer several advantages. These include the ability to directly validate satellite-derived wind speed at hub height. Satellite-based estimates typically derive the wind speed at hub height indirectly, using surface roughness to estimate the wind speed at 10 m and subsequently extrapolating to hub height. Airborne measurements also complement the spatial coverage provided by long-range scanning wind lidar systems, 165 which are typically fixed at a single location and can retrieve wind field data over distances of up to approximately 15 km,

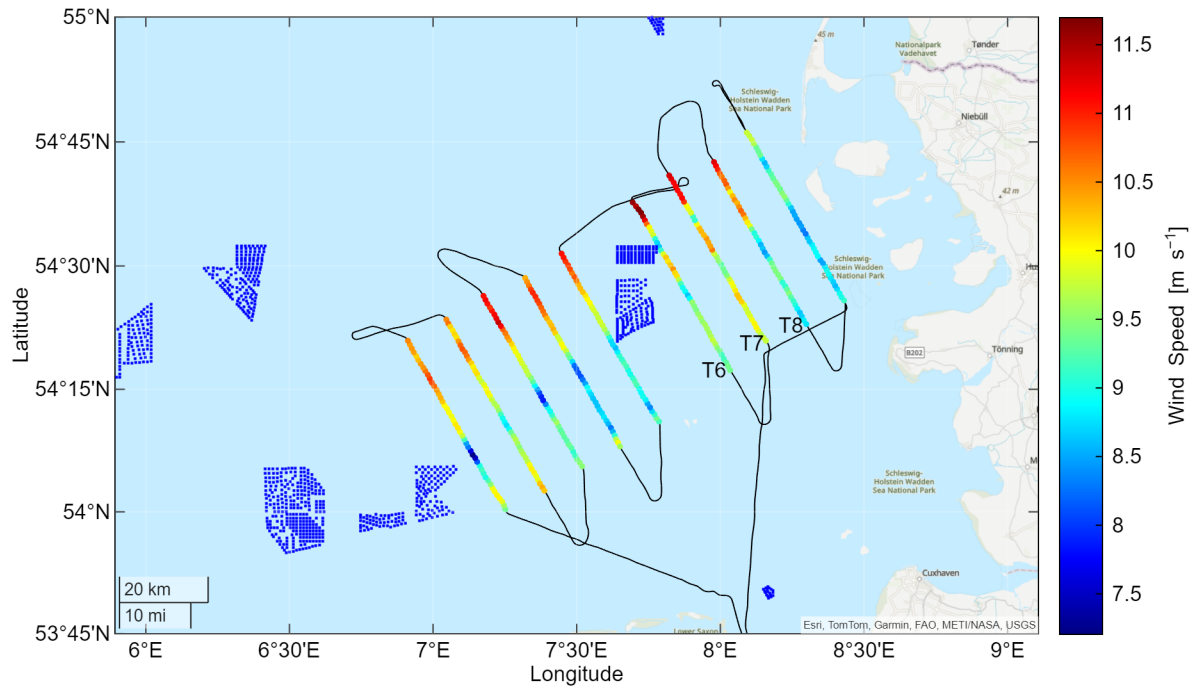


Figure 2. In-situ wind speed measured on 11 September 2021 by the research aircraft D-IBUF from 12:51 UTC to 17:13 UTC in the lee of wind farm clusters N2 and N3 for South-Westerly wind direction. Blue dots represent the individual wind turbines, black lines represent the flight path of the aircraft. Wind speed measurements along the flight path are colour coded and plotted for every 15 s. The indicated transects through the wakes T6, T7 and T8 are used for direct comparison with satellite data in Fig. 3. Powered by Esri.

depending on atmospheric conditions. The effective range of these systems is influenced by several factors, including aerosol concentration (which influences backscatter strength), atmospheric visibility and humidity (which affect signal attenuation), laser pulse energy and optical design (which influence system sensitivity), and the scanning geometry (as longer path lengths or steeper elevation angles can reduce the signal-to-noise ratio). In contrast, point measurements from fixed installations such 170 as the FINO1 meteorological mast (FINO1, 2025) provide data with high precision and high resolution in time, but are limited to single locations where additional measurements are needed to estimate wake strengths.

3.2 Wake interaction

The overlap and interaction of different wind farm wakes have been investigated by numerical simulations of different complexity (Cañadillas et al., 2020; Cañadillas et al., 2023; Foreman et al., 2024; Sengers et al., 2024) and by satellite images 175 providing an overview of large scales (Djath et al., 2018). Fig. 4 shows airborne measurements which confirm the further reduction of the wind speed downstream of a second wind farm, with the wind speed reduction depending on turbine density

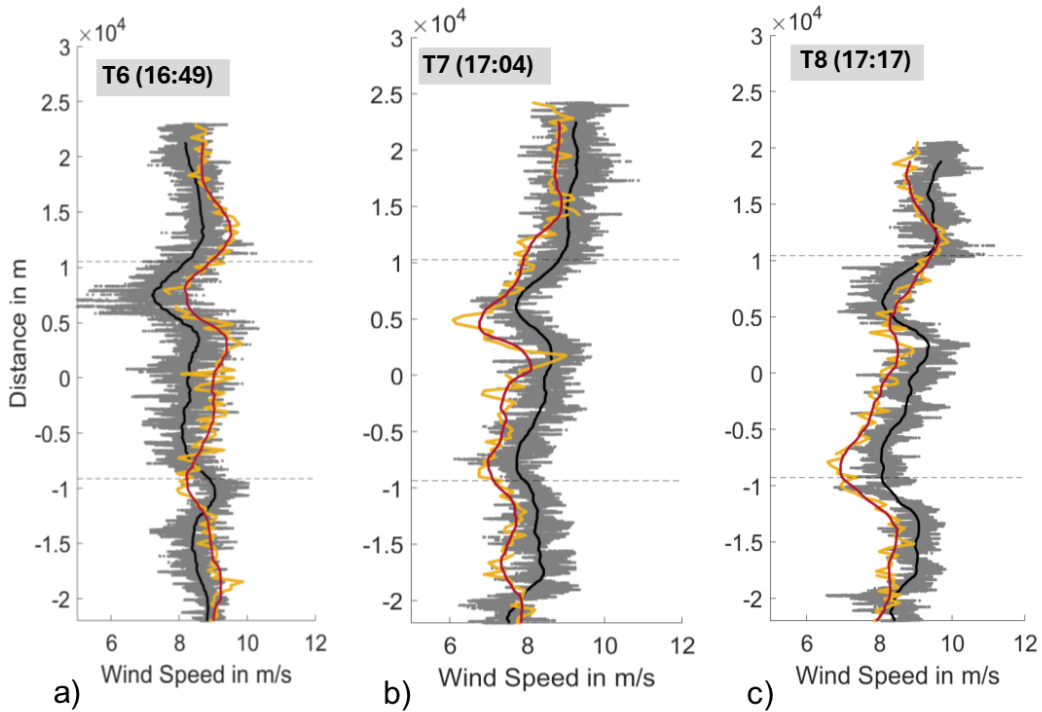


Figure 3. Comparison of airborne wind measurements of D-IBUF (running mean, black) showing substantial small-scale variability (gray shading) with collocated SAR-derived wind speed (red) and variability (yellow) on 11 September 2021. The SAR wind speed was extrapolated from an altitude of 10 m to hub height using stability information obtained from the flight. Panels (a), (b), and (c) correspond to different sampling times (in UTC) and transects called T6, T7 and T8 of the flight data.

and the mode of operation (Cañadillas et al., 2022; zum Berge et al., 2024). In addition, a wind farm not in operation does induce downstream turbulence, even if the wind speed is not reduced significantly (zum Berge et al., 2024). Building on these findings, zum Berge et al. (2024) evaluated both engineering and mesoscale models using the in situ airborne measurements

180 behind large-scale wind farm clusters in the German Bight. The study compared four representative measurement flights with simulations from the Weather Research and Forecasting Model (WRF), developed by the National Center of Atmospheric Research widely used in the wind energy community (Skamarock et al., 2019), including wind farm parameterizations and several engineering wake models implemented in the FOXES software tool (Schmidt et al., 2023). Results showed that engineering models, when properly configured or coupled with mesoscale input, are capable of reproducing wake effects over tens of kilo-
 185 metres, including merged wakes from multiple farms. Particularly, the engineering model coupled with WRF — where turbine wakes are propagated along flow streamlines derived from WRF simulations (zum Berge et al., 2024) — proved to be most consistent with the airborne observations, especially under stable stratification. However, all models showed reduced performance further downstream, highlighting the importance of accurate inflow conditions and atmospheric stability characterization. The study underlines the value of high-resolution airborne data for benchmarking wake models in clustered offshore wind farm

190 environments.

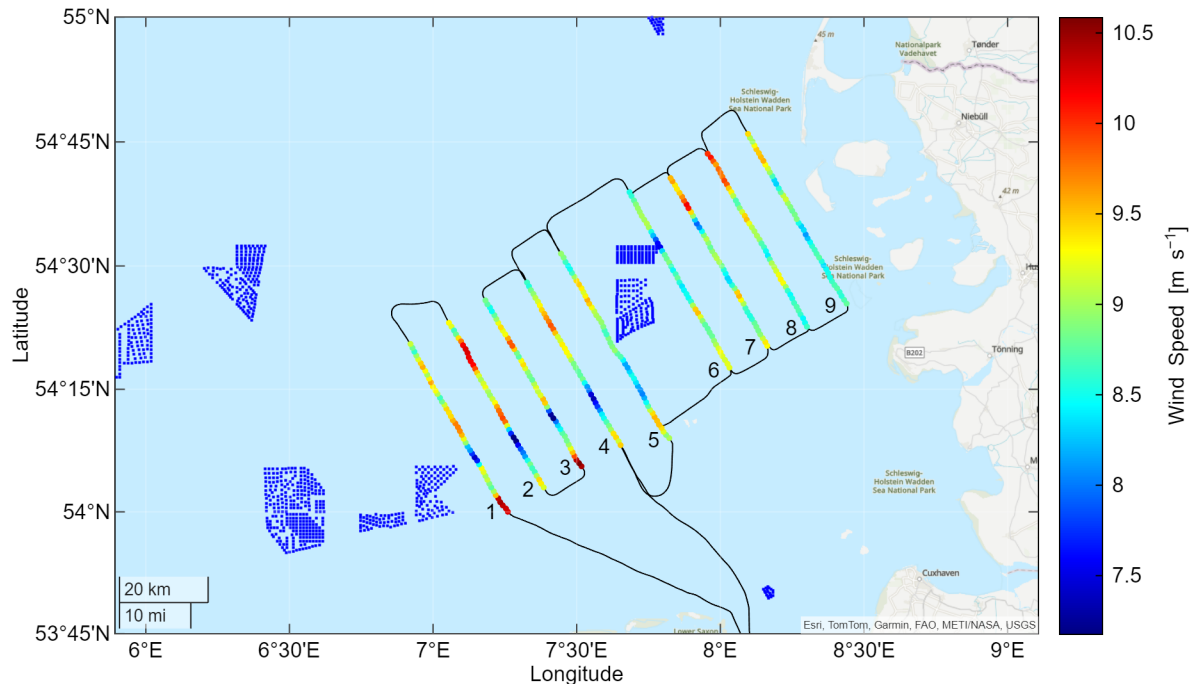


Figure 4. Wind speed measured at hub height in-situ by the research aircraft D-IBUF in the lee of wind farm clusters N2 and N3 for southwesterly wind direction on 27 July 2021. Blue dots represent the wind farm cluster, black lines represent the flight path of the aircraft. Wind speed measurements along the flight path are colour coded and plotted for every 15 s. Powered by Esri.

3.3 Modification of latent heat fluxes

Airborne measurements were able to show that latent heat fluxes increased above and downstream of wind farm clusters across a range of atmospheric stability regimes (Platis et al., 2023). Under thermally stable conditions, nearly all flights showed a 195 notable increase in upward latent heat flux above the wind farms, with maximum enhancements reaching $+160 \text{ W m}^{-2}$ relative to background conditions. During near neutral stratification, the latent heat flux enhancement was generally stronger, with peak values up to $+600 \text{ W m}^{-2}$, although more spatially confined. The data suggest that while the signal is more consistently detectable during stable conditions, it becomes more pronounced under neutral conditions. This is likely due to enhanced vertical mixing induced by the wind farms, which facilitates downward entrainment of drier air into the near-surface layer, 200 enhancing the evaporation potential. The increase in latent heat flux was generally limited to the area above and immediately



downstream (up to around 1 km) of the wind farms (Fig. 5), while the associated wakes extended further downwind, indicating different spatial scales of momentum and scalar flux modifications.

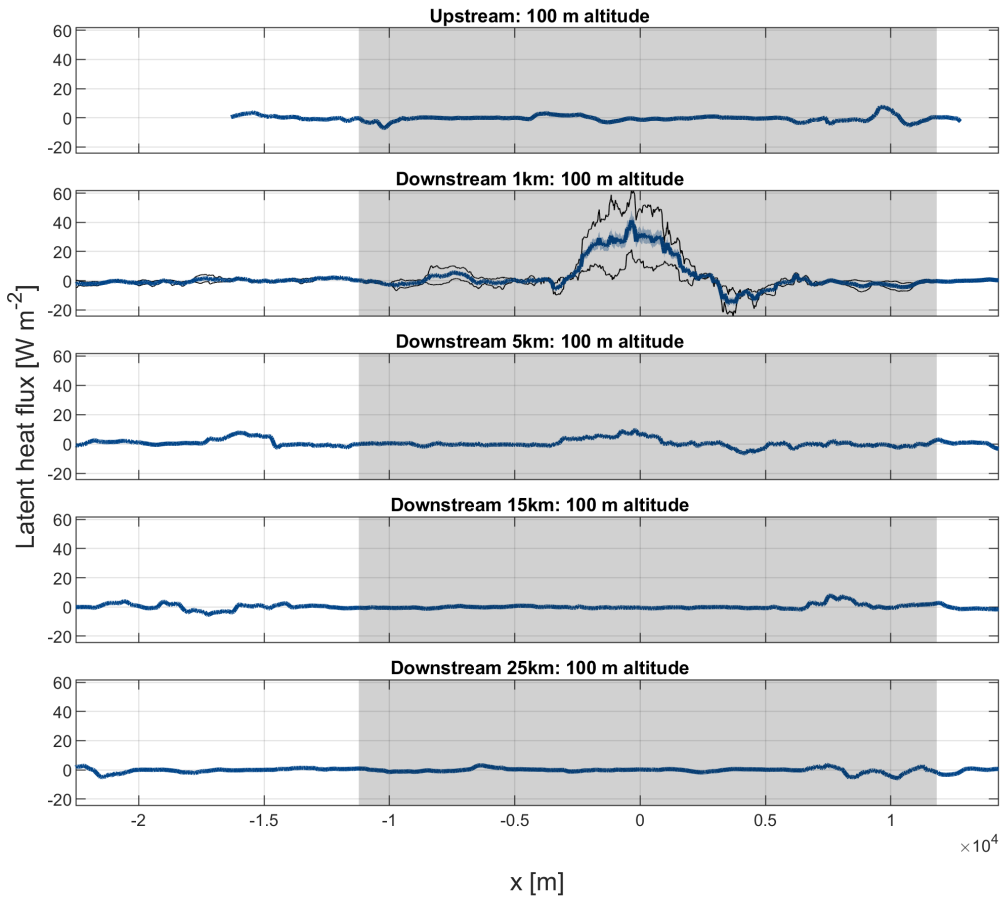


Figure 5. Airborne observations obtained with D-IBUF of the turbulent latent heat flux on 27 May 2017 during a research flight at the Amrumbank West wind farm cluster N4. Measurements were taken upstream and downstream of the cluster under weakly stable thermal stratification, with a capping inversion located at around 800 m above sea level. The figure presents the latent heat flux collected along two consecutive flight legs aligned perpendicular to the prevailing wind direction of 130 degree and flown at hub height (100 m). The blue line represents the averaged latent heat flux across both flight legs, while the grey-shaded area indicates the projected position of the Amrumbank West wind farm along the mean wind direction. The blue-shaded envelope denotes the measurement uncertainty associated with the latent heat flux. The figure has been published in Platis et al. (2023).

However, attributing the observed effects solely to wind farm influence remains also challenging for airborne observations due to varying flight patterns, measurement altitudes, atmospheric background variability, and limitations in a suitable definition for accurately classifying stability (Platis et al., 2021). Additionally, wind farm characteristics such as turbine layout and



density likely play a role in modulating the magnitude of these impacts. The observed modification of moisture fluxes at hub height and above suggests potential downstream effects on surface latent heat fluxes, as supported by previous numerical modelling studies. While our measurements represent only short-term snapshots, they support the hypothesis that offshore wind farms may locally alter the surface energy budget and atmospheric structure (Platis et al., 2023). For instance, on two flights 210 with near-saturated humidity and weakly stable conditions, small cumulus clouds were visually observed forming directly above wind farms, suggesting that increased latent heat flux may contribute to localized cloud development.

3.4 Coastal effect

The wind speed over the North Sea is typically higher than over land due to the lower surface roughness, which is approximately two orders of magnitude lower over water (Taylor, 1970; Lange et al., 2004), and the higher heat capacity of water. However, 215 the transition of wind from land to sea, and the distance required to reach an equilibrium wind speed, is strongly influenced by atmospheric stability (Djath et al., 2022), the formation of internal boundary layers (Barekzai et al., 2025a, b), and mesoscale phenomena such as low-level jets (LLJ) (Djath et al., 2022) and sea breezes. Previous studies (e.g., Schulz-Stellenfleth et al., 2022; Djath et al., 2022; Cañadillas et al., 2023) show that offshore wind speed generally increases with distance from the coast, especially at lower altitudes. This increase is more pronounced under neutral or unstable conditions and is attenuated at 220 higher altitudes. Atmospheric stratification plays a critical role: stable conditions can delay the offshore wind adjustment, while unstable conditions tend to accelerate it. For studies in the German Bight, the equilibrium was typically reached within 50-80 km. A mesoscale modelling study over the Baltic Sea showed potential temperature developments under stable stratification over distances of more than 200 km (Dörenkämper et al., 2015).

Cañadillas et al. (2023) present two contrasting measurement flights that highlight this behaviour (Fig. 6). On 23 July 2020, 225 offshore warming (increase of surface temperature in the early morning, from 13°C above land to 17°C at FINO1) resulted in reduced atmospheric stability and enhanced vertical mixing, leading to the dissipation of a land-based LLJ and an increase in wind speed with fetch. In contrast, on 23 September 2020, a strong inland stratification weakened gradually offshore, resulting in a breakdown of the LLJ and deceleration of wind with distance from the coast. The airborne data were analysed in the context of stationary lidar measurements at the island of Norderney (Rausch et al., 2023b) and at the meteorological mast FINO1, as 230 well as satellite observations, and complemented with ERA5 reanalyses data and WRF simulations (Cañadillas et al., 2023). These cases illustrate the complexity and height-dependence of coastal wind transitions and underscore the importance of resolving mesoscale processes in offshore wind assessments. Airborne measurements are a suitable tool to study these effects of coastal transition.

3.5 Evaluation of numerical flow simulations

235 Airborne measurements offer significant potential for capturing atmospheric parameters during periods with meteorologically interesting flow conditions (e.g., stable stratification around and above offshore wind farms), which can be compared to simulations. Unlike many ground-based methods, they provide high-resolution data in both horizontal and vertical directions, often exceeding 1000 m in altitude. This makes them a valuable tool for comparison with simulations and for evaluating parameter-

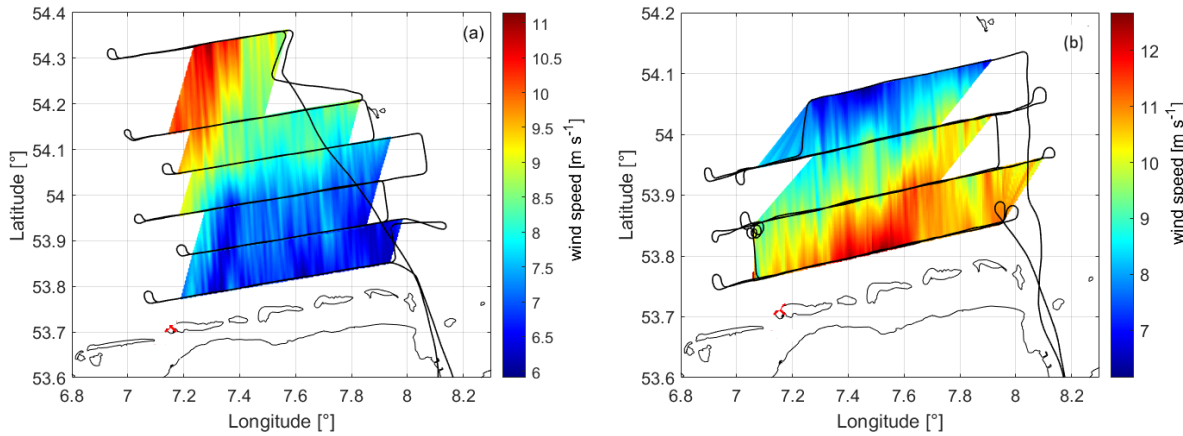


Figure 6. Contour plot of interpolated aircraft D-IBUF wind field measurements along the mean wind direction from South at 100 m altitude, with the black line indicating the flight trajectory from 07:05 to 11:03 UTC on 23 July 2020 (a) and from 05:24 to 08:53 UTC on 23 September 2020 (b), as published in Cañadillas et al. (2023).

izations in numerical models, including those related to wind turbines and turbulence, particularly in complex flow regimes
 240 such as those found in offshore environments, e.g., Siedersleben et al. (2018a); Platis et al. (2020); Cañadillas et al. (2023).

3.5.1 Mesoscale simulations

Mesoscale simulations, such as those performed with WRF, experience intrinsic difficulties of direct comparison with single observations as provided by the different flights. WRF simulations suffer from time shifts (zum Berge et al., 2024) and an overall lack of detailed accuracy, when single situations are considered. In particular, WRF simulations have generally shown
 245 difficulties in accurately representing atmospheric stability (Siedersleben et al., 2018a, b). These discrepancies are particularly pronounced near coastal regions, where deviations are larger compared to offshore locations over open water (Platis et al., 2020). Under stable conditions, the model struggles to accurately reproduce the altitude of the inversion layer (Siedersleben et al., 2020), as well as the coastal transition zone (Cañadillas et al., 2023). The WRF model, using the wind farm parameterization by Fitch et al. (2012), was found to capture the horizontal extent of wakes well (Cañadillas et al., 2022), even under
 250 stable conditions. However, it struggled to accurately reproduce the absolute wind speed. Both observations and simulations consistently show that the wind speed deficit extends above the upper tip height of the rotor (Siedersleben et al., 2018a). Several studies have used the airborne dataset to first evaluate model performance and subsequently draw conclusions on wake behaviour and model representation (Larsen and Fischereit, 2021; van Stratum et al., 2022; Ali et al., 2023).

Simulation progress has been achieved by coupling atmospheric and oceanic models. The mechanism for creating turbulence
 255 for wind turbines does not seem to be constant with height to reproduce observations (Larsen et al., 2024).

First modelling experiments indicate that the angle between wind and wave direction plays a role for the undisturbed wind profile upstream of wind farms, as aligned wind-wave directions result in a lower roughness length. This reduced friction leads to



higher wind speed. Further, the angle between wind and wave direction influences the wind speed recovery in the downstream wakes, as opposing wind and wave direction lead to more vertical mixing and therefore shorter wakes (Porchetta et al., 2021; 260 Christiansen et al., 2022; Schmitt et al., 2025).

3.5.2 Engineering Models

Engineering models, such as FLORIS (Gebraad et al., 2016), PyWake (Pedersen et al., 2023), Open Wind (OpenWind , 2020) and FOXES (Schmidt et al., 2023), are widely used to optimize wind farm layouts and estimate energy production. Since this 265 optimization process requires a large number of simulations across various configurations, the underlying wake models must be computationally efficient. Consequently, the flow within and around wind farms is typically strongly simplified by analytical, e.g., Gaussian models that describe the wake decay downstream of individual turbines, which are then superposed (Cañadillas et al., 2023). Engineering models are apparently working only on average. While it is possible to collect measurements with the aircraft over multiple days, there is a lot of scatter in the measured wind speed values. Hence, with such large standard 270 deviations, comparison to engineering models is generally challenging.

Despite their focus on representing the annual energy production in the long-term correctly, several studies have used two-dimensional airborne measurements to compare wake recovery behind offshore wind farms with engineering model results. For example, Cañadillas et al. (2020) analysed data from a series of flights conducted within the wakes at various distances downstream of two wind farm clusters in the North Sea under different atmospheric stability conditions. The study concluded 275 that engineering models, which are often configured for neutral conditions, tend to underestimate wake effects under stable stratification.

In a more recent study, zum Berge et al. (2024) applied several WRF and engineering models with different configurations, WRF with a wind farm parameterization (WRF-WF), an engineering model coupled to WRF (EM-WRF), a standard engineering model with a baseline calibration (EM-BL), a calibration aiming at strongly dampening wake recovery (EM-LR), and the TurbOPark model (Pedersen et al., 2022) of Ørsted (EM-TP) to simulate large-scale cluster wakes over extended distances in 280 the German Bight and compared the results with airborne measurements. Fig. 7, reproduced from zum Berge et al. (2024), shows the comparison of measured and modelled wake recovery for a large offshore wind farm cluster. Overall, the engineering models showed good agreement with the observations in the immediate vicinity of the wind farms and up to 20–30 km downstream. However, their accuracy in predicting the wake induced wind speed deficit declined significantly with increasing distance from the wind farm clusters.

285 3.6 Sea state

As wind is a driving force for sea state development, the reduced wind speed downstream of wind farms leads to changes in the wave spectra. The enhanced laser scanner surface reflectance in wake areas (Platis et al., 2018) indicates that the water surface is smoother, and a larger percentage of the laser pulse is reflected back to the receiver. These changes of the surface roughness can take place on the horizontal scale of less than 1 km. Modifications of the wave spectra, i.e., the energy per wavelength, 290 were observed in wake areas for developing sea state conditions (Bärfuss et al., 2020).

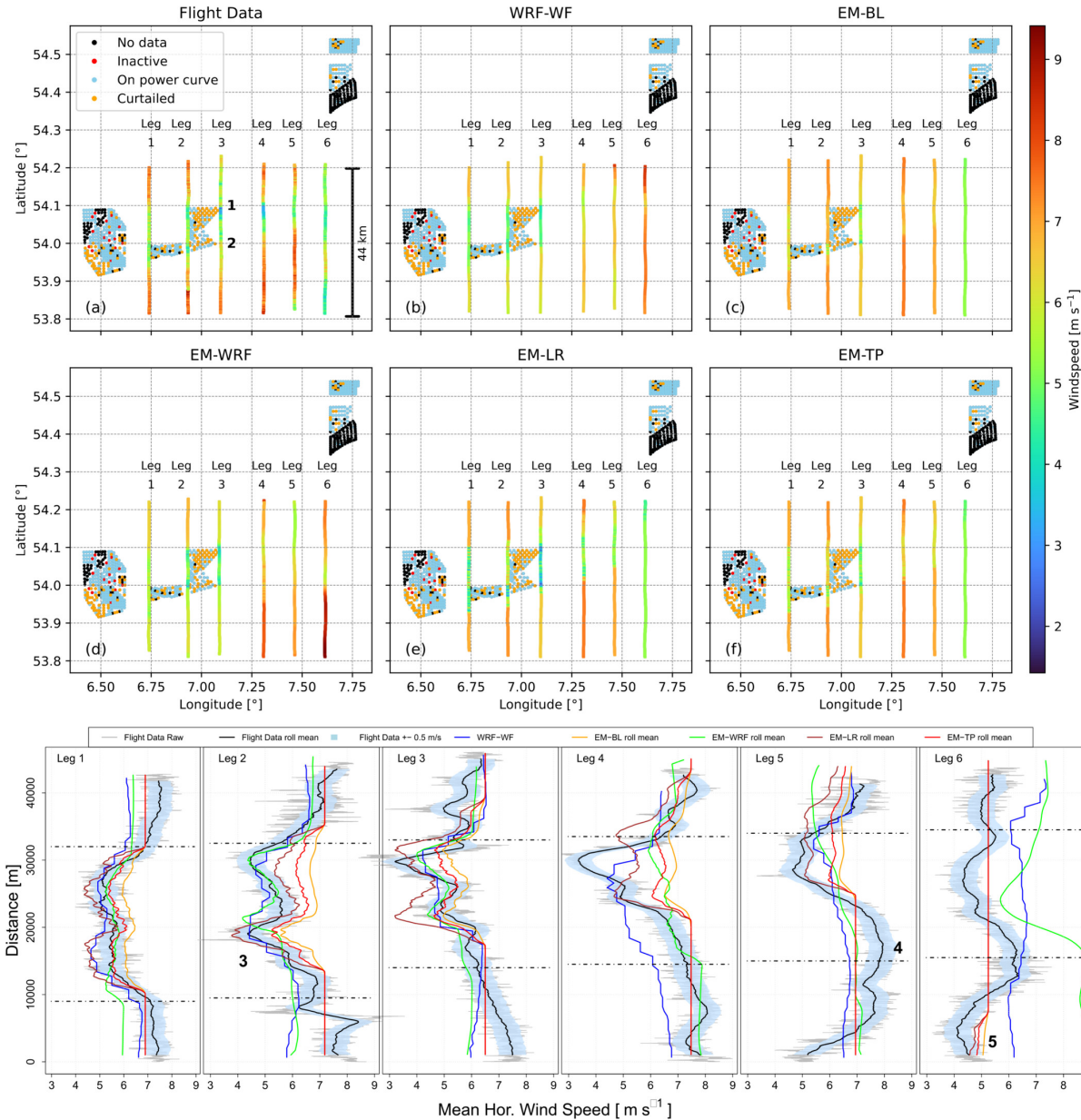


Figure 7. Top part: the measurement area in the German Bight with wind farm clusters N2, N3, and N4 on 14.07.2020 between 12:30 and 16:00 UTC. The dots represent the individual turbines and their operational status during the entire measurement time. (a) Results of the flight measurements on six flight legs with a mean wind direction of 270°. Results of the model calculations on the coordinates of the flight paths corresponding to (b) WRF-WF, (c) EM-BL, (d) EM-WRF, (e) EM-LR, and (f) EM-TP. Bottom part: The flight legs are shown as line plots with running mean values for direct comparison. The dashed lines represent the estimated wake area. Graphic reproduced from zum Berge et al. (2024) (Figure 7), licensed under CC BY-NC-ND 4.0 <https://creativecommons.org/licenses/by-nc-nd/4.0/>.

A significant reduction in wind speed in the wake of a wind farm also results in a decrease in significant wave height. Under stable atmospheric conditions, influences on sea state characteristics can be detected that can be attributed to a sea surface wake induced by the atmospheric wake. For the atmospheric wake, different parameters such as wind speed reduction are characteristic for the wake length. Characteristics for the sea surface wake can be selected as well. A simple, yet meaningful description can be provided by the reduction of the significant wave height. More detailed analyses can be performed using the spectral sea surface energy distribution. Figure 8 shows such an energy distribution of the measurement flight on 24 July 2020. The area influenced by the wind farm is depicted within the black lines, and from a graphical perspective, the wind originates from the left, i.e., from 270° . Within the black lines, a reduction in wind speed is observed which can be noted as the wake of the wind farm. As the wind speed decreases, the energy density spectrum is also modified over a wide frequency range. This can be observed to a downstream distance of at least 25 km behind the wind farm. Wind farms can have a significant impact on developing sea state conditions, particularly on young wind waves. Reduced wind speed disrupts wave growth, resulting in a less energetic spectrum. A larger impact on sea conditions is observed for stable atmospheric conditions with more pronounced reductions in wind speed.

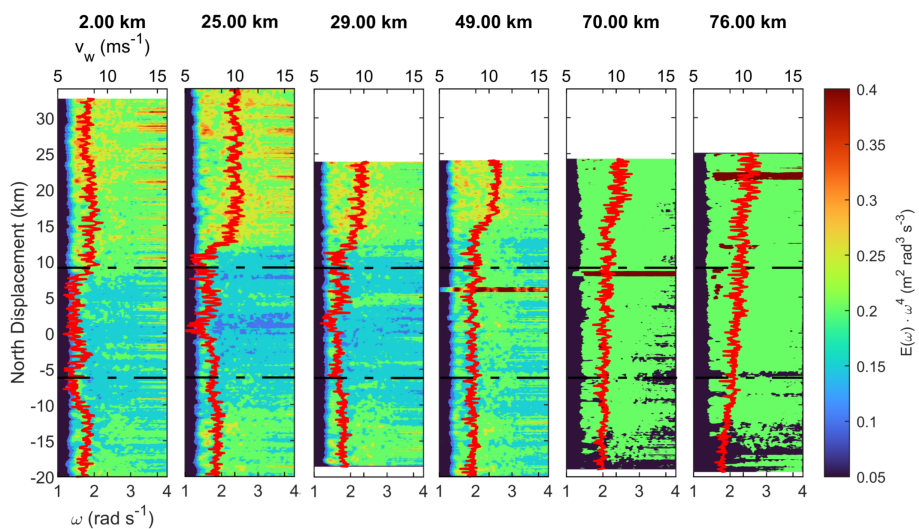


Figure 8. Sea surface energy distribution (colour-coded) for the flight on 24 July 2020 downstream of the wind farm clusters N2/N3 with stable atmospheric conditions. The airborne measured wind speed is represented by the red lines. On that day, wind originated from 270° with a mean velocity of 10 m s^{-1} . The estimated wake region is depicted by the dashed lines. The horizontal, narrow lines with high energy density can be attributed to boats or other disturbances near the sea surface. For each subplot, the downstream distance from the wind farm cluster is provided.



3.7 Global blockage effect

305 The global blockage effect (GBE) is the combined induction zone of all turbines in a wind farm (Porté-Agel et al., 2020). The upstream pressure field is responsible for deflecting the upstream flow to the side (Schneemann et al., 2025) and above the wind farm (Porté-Agel et al., 2020). The upward deflection reaches the upper atmospheric layers where stable stratification is always present and thus induces gravity waves that further intensify the GBE (Centurelli et al., 2021; Lanzilao and Meyers , 2024).
310 Therefore, GBE depends on atmospheric boundary layer height and stratification of the inversion layer and the free atmosphere (Lanzilao and Meyers , 2024). Schneemann et al. (2021) also demonstrate that the GBE is sensitive to the stratification of the atmospheric boundary layer, as justified by Sanchez Gomez et al. (2023). It is still subject of research if and to which extend it leads to a net power loss in a wind farm or rather a power redistribution (Lanzilao and Meyers , 2024). Compared to wind turbine or wind farm wake effects the GBE is much harder to investigate experimentally (Meijer et al., 2024). While wind speed gradients in wind farm wakes appear in the order of m s^{-1} over short distances of some hundreds of metres (Schneemann 315 et al., 2020), the wind speed gradient in GBE spreads over distances of several kilometres with much smaller wind speed differences of only tenths of m s^{-1} (Schneemann et al., 2021). Similar to the previously described downstream wind farm wake investigations, airborne measurements with horizontal flight legs were performed upstream of wind farms. The flight path was oriented perpendicular to the main wind direction with the goal to quantify GBE induced wind speed differences in front of and beside the farm. The investigations were limited by the flight permission, which only allowed to operate with a 320 safety distance of at least 500 m to the wind turbines.

Figure 9 shows an exemplary data set and illustrates how the GBE was investigated: The flight patterns were aligned close to the wind farm cluster N4 with distances of 500 m to 2 km upstream. The wind speed was normalized to 1 in the undisturbed areas next to the areas affected by wakes, and latitudinal and longitudinal transects are displayed. Based on all flights with such patterns, small average numbers of wind speed reductions in the wake areas compared to the undisturbed areas were 325 observed in the range of 2% for the closest flight distance of 500 m with a high scatter. On averaged data, a not significant trend of reduced wind speed in the direction towards the farm is visible, which cannot be reliably attributed to GBE. In this overview, different days with different atmospheric conditions are compared. The wind speed difference is calculated over large distances not considering mesoscale changes in the wind field. In summary, it turned out that the GBE is potentially too small to be determined by airborne measurements for single flights.

330 4 Conclusions

In conclusion, aircraft measurements provide many advantages for wind energy investigations: They can be flexibly adapted to the wind direction to study wake effects. They provide highly resolved data of air temperature, humidity, and wind speed and direction. This allows for vertical profile measurements to obtain a detailed description of the local atmospheric boundary layer, including the derivation of atmospheric stability as well as high resolution horizontal measurements to quantify atmospheric 335 structures spanning over large areas. Simultaneous measurements of atmospheric modifications and changes in the surface properties can be recorded. The extensive data sets of the research projects WIPAFF and X-Wakes are to date unique for

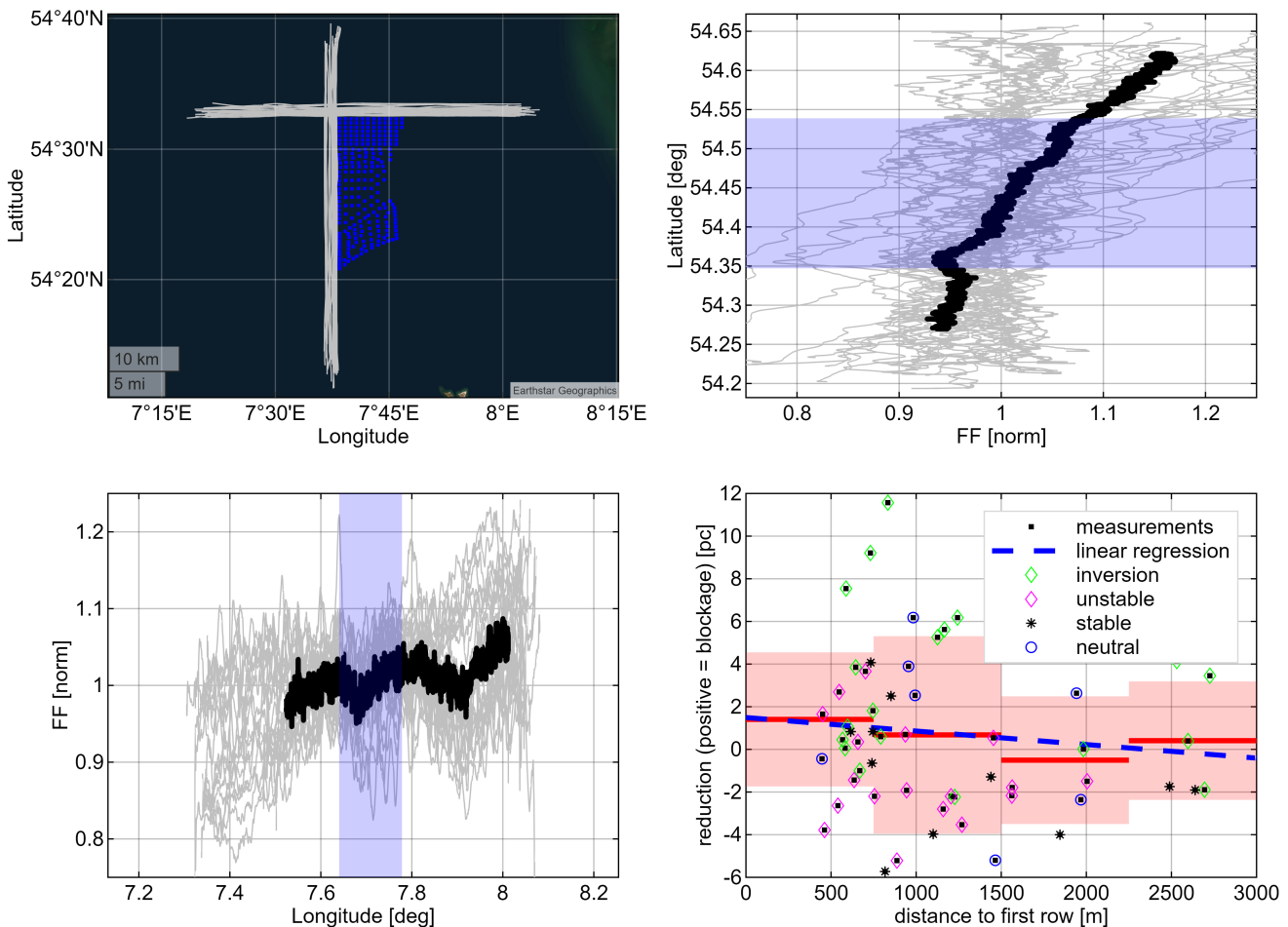


Figure 9. Airborne investigation of the blockage effect for wind from North and West. Upper left: flight sections (in white) used for investigation of the blockage effect around the wind farms (single wind turbines in blue). The sections were flown on different days and at different distances in front of the first wind turbine row. Upper right: This panel shows the unfolding of all meridional measurement sections on latitude vs. normalised wind speed (normalised by the median wind speed outside the wake for the leg regarded). The averaged normalised wind speed is shown with a thick black line. Lower left: This panel shows the unfolding of all longitudinal measurement sections on longitude vs. normalised wind speed (normalised by the median wind speed outside the wake for the leg regarded). The averaged normalised wind speed is shown with a thick black line. Lower right: Statistical results: relative wind speed reduction which could be caused by the GBE over measurement leg distance. The single measurement legs used for the analysis are shown as black dots, with an overlaying marker for inversion/unstable/stable and neutral conditions. Average relative wind speed reduction is shown as red line for each distance band, with an underlying reddish region indication standard deviation (1σ). The dashed blue line is the first order polynomial regression on average relative wind speed reduction versus distance to the first row of the wind turbines.



flexibly characterizing the North Sea atmospheric boundary layer. There is a large potential of combining the airborne data with satellite investigations, stationary long-term measurements by meteorological masts or lidar systems and numerical simulations. Therefore, the airborne data sets obtained during the projects WIPAFF (Bärfuss et al., 2019; Lampert et al., 2020) and X-340 Wakes (Rausch et al., 2023a; Lampert et al., 2024) provide a valuable base for investigating offshore wind conditions and their interaction with wind farms.

Data availability. The airborne meteorological data of the project WIPAFF are published in Bärfuss et al. (2019), and the data of the project X-Wakes in Rausch et al. (2023a)

345 *Author contributions.* AL wrote the initial draft of the manuscript with contributions from all co-authors. AL, BC, JSS, JB, JS, TN, MD, BS, SE, MK, HH, DH, JP, and AP designed the project idea and acquired funding. All authors worked with the airborne data sets and performed different studies quoted in the manuscript.

Competing interests. One of the authors is a member of the Editorial Board. The other authors declare no competing interests.

350 *Acknowledgements.* The projects WIPAFF and X-Wakes were funded by the German Federal Ministry for Economic Affairs and Energy under grant number 0325783 and 03EE3008, respectively, on the basis of a decision by the German Bundestag. The authors would like to thank the aircraft crew, Rolf Hankers, Thomas Feuerle, Mark Bitter, Helmut Schulz, Matthias Cremer, Maik Angermann and Jonas Füllgraf, for making it possible to acquire the airborne data above the North Sea.



References

Abkar, M., Sharifi, A., and Porté-Agel, F.: Wake flow in a wind farm during a diurnal cycle, *J. of Turbulence*, 17, 4., 420-441, 355 <http://dx.doi.org/10.1080/14685248.2015.1127379>, 2016.

Akhtar, N., Geyer, B., Rockel, B., Sommer, P.S., and Schrum, C.: Accelerating deployment of offshore wind energy alter wind climate and reduce future power generation potentials, *Nature Sci. Rep.*, 11, 11826, <https://doi.org/10.1038/s41598-021-91283-3>, 2021.

Akhtar, N., Geyer, B., and Schrum, C.: Impacts of accelerating deployment of offshore windfarms on near-surface climate, *Nature Sci. Rep.*, 12, 18307, <https://doi.org/10.1038/s41598-022-22868-9>, 2022.

360 Ali, K., Schultz, D.M., Revell, A., Stallard, T., and Ouro, P.: Assessment of five wind-farm parameterizations in the Weather Research and Forecasting model: A case study of wind farms in the North Sea, *Monthly Weather Review*, DOI: 10.1175/MWR-D-23-0006.1, 152, 9, 2333–2359, 2023.

Anantharaman, A., Schneemann, J., Theuer, F., Beaudet, L., Bernard, V., Deglaire, P., and Kühn, M.: The impact of far-reaching offshore cluster wakes on wind turbine fatigue loads, *Wind Energ. Sci.*, 10, 1849–1867, <https://doi.org/10.5194/wes-10-1849-2025>, 2025.

365 Barekzai, M., Cañadillas, B., Emeis, S., Dörenkämper, M., and Lampert, A.: Mesoscale Simulations of Coastal Boundary-Layer Transitions. Part 1: Low-Level Jets, *Meteorologische Zeitschrift*, 33, 6, 457-474, DOI: 10.1127/metz/2024/1195, 2025.

Barekzai, M., Cañadillas, B., Emeis, S., Dörenkämper, M., and Lampert, A.: Mesoscale Simulations of Coastal Boundary-Layer Transitions. Part 2: Offshore Wind Speed Development, *Meteorologische Zeitschrift*, 33, 6, 475 - 488, DOI: 10.1127/metz/2024/1196, 2025.

Bärfuss, K., Hankers, R., Bitter, M., Feuerle, T., Schulz, H., Rausch, T., Platis, A., Bange, J., and Lampert, A.: In-situ air-370 borne measurements of atmospheric and sea surface parameters related to offshore wind parks in the German Bight, PANGAEA, <https://doi.pangaea.de/10.1594/PANGAEA.902845>, 2019.

Bärfuss, K., Djath, B., Lampert, A., and Schulz-Stellenfleth, J.: Airborne LiDAR Measurements of the sea surface properties in the German Bight, *IEEE Transactions on Geoscience and Remote Sensing*, doi: 10.1109/TGRS.2020.3017861, 2020.

Bärfuss, K., Schulz-Stellenfleth, J., and Lampert, A.: The Impact of Offshore Wind Farms on Sea State Demonstrated by Airborne LiDAR 375 Measurements, *J. Mar. Sci. Eng.* 2021, 9, 644, 2021.

Bärfuss, K. B., Schmithüsen, H., and Lampert, A.: Drone-based meteorological observations up to the tropopause – a concept study, *Atmos. Meas. Tech.*, 16, 3739–3765, <https://doi.org/10.5194/amt-16-3739-2023>, 2023.

Bastankhah, M., and Porté-Agel, F.: A new analytical model for wind-turbine wakes, *Renewable Energy*, 70, 116-123, <https://doi.org/10.1016/j.renene.2014.01.002>, 2014.

380 Bailey, H., Brookes, K.L., and Thompson, P.M.: Assessing environmental impacts of offshore wind farms: lessons learned and recommendations for the future, *Aquatic Biosystems*, 10, 1-13, 2014.

zum Berge, K., Centurelli, G., Dörenkämper, M., Bange, J., and Platis, A.: Evaluation of Engineering Models for Large-Scale Cluster Wakes With the Help of In Situ Airborne Measurements, *Wind Energy*, 27, 1040–1062, <https://doi.org/10.1002/we.2942>, 2024.

Bleeg, J., Purcell, M., Ruisi, R., and Traiger, E.: Wind Farm Blockage and the Consequences of Neglecting Its Impact on Energy Production. 385 Energies, 11, 6, 1609, <https://doi.org/10.3390/en11061609>, 2018.

Bodini, N., Lundquist, J.K., and Moriarty, P.: Wind plants can impact long-term local atmospheric conditions, *Sci. Rep.*, 11, 1, 1-12, 2021.

Broström, G.: On the influence of large wind farms on the upper ocean circulation, *Journal of Marine Systems*, 74, 585–591, <https://doi.org/10.1016/j.jmarsys.2008.05.001>, 2008.



Cañadillas, B., Foreman, R., Barth, V., Siedersleben, S., Lampert, A., Platis, A., Djath, B., Schulz-Stellenfleth, J., Bange, J., Emeis, S., and
390 Neumann, T.: Offshore wind farm wake recovery: Airborne measurements and its representation in engineering models, *Wind Energy*, doi:10.1002/we.2484, 17 pp., 2020.

Cañadillas, B., Beckenbauer, M., Trujillo, J.J., Dörenkämper, M., Foreman, R., Neumann, T., and Lampert, A.: Offshore wind farm cluster
wakes as observed by long-range-scanning wind lidar measurements and mesoscale modeling, *Wind Energy Science*, 7, 1241-1262, 2022.

Cañadillas, B., Wang, S., Ahlert, Y., Djath, B., Barekzai, M., Foreman, R., and Lampert, A.: Coastal horizontal wind speed gradients in the
395 North Sea based on observations and ERA5 reanalysis data, *Meteorologische Zeitschrift*, 32(3), 207–228, doi:10.1127/metz/2022/1166,
2023.

Cañadillas, B., Foreman, R., Steinfeld, G., and Robinson, N.: Cumulative interactions between the global blockage and wake effects as ob-
served by an engineering model and large-eddy simulations, *Energies*, 16(7), 2949, <https://doi.org/10.3390/en16072949>, 2023. Available
at: <https://www.mdpi.com/1996-1073/16/7/2949>.

400 Centurelli, G., Vollmer, L., Schmidt, J., Dörenkämper, M., Schröder, M., Lukassen, L.J., and Peinke, J.: Evaluating Global Blockage engineer-
ing parametrizations with LES, *J. Phys.: Conf. Ser.*, 1934, 012021, 2021.

Christiansen, M.B., and Hasager, C.B.: Wake effects of large offshore wind farms identified from satellite SAR, *Remote Sens. Env.*, 98,
251-268, 2005.

Christiansen, N., Daewel, U., and Schrum, C.: Tidal mitigation of offshore wind wake effects in coastal seas, *Frontiers in Marine Science*, 9,
405 1006647, doi:10.3389/fmars.2022.1006647, 2022.

Christiansen, N., Daewel, U., Suzuki, N., Carpenter, J.R., and Schrum, C.: Regional modeling of structure-induced mixing at offshore wind
farm sites, *Front. Mar. Sci.*, 10, 2023a.

Corsmeier, U., Hankers, R., and Wieser, A.: Airborne turbulence measurements in the lower troposphere onboard the research aircraft Dornier
128-6, D-IBUF, *Meteorol. Z.*, 10, 315–329, 2001.

410 Daewel, U., Akhtar, N., Christiansen, N., and Schrum, C.: Offshore wind farms are projected to impact primary production and bottom water
deoxygenation in the North Sea, *Communications Earth and Environment*, 3, 292, <https://doi.org/10.1038/s43247-022-00625-0>, 2022.

Djath, B., Schulz-Stellenfleth, J., and Cañadillas, B.: Impact of atmospheric stability on X-band and C-band synthetic aperture radar imagery
of offshore windpark wakes. *J. Renewable Sustainable Energy*, 10, 4, 043301, <https://doi.org/10.1063/1.5020437>, 2018.

Djath, B., Schulz-Stellenfleth, J., and Cañadillas, B.: Study of Coastal Effects Relevant for Offshore Wind Energy Using Spaceborne Syn-
415 thetic Aperture Radar (SAR). *Remote Sens.* 2022, 14, 1688. <https://doi.org/10.3390/rs14071688>, 2022.

Dörenkämper, M., Witha, B., Steinfeld, G., Heinemann, D., and Kühn, M.: The impact of stable atmospheric boundary lay-
ers on wind-turbine wakes within offshore wind farms, *J. Wind Engineering and Industrial Aerodynamics*, 144, 146-153,
<https://doi.org/10.1016/j.jweia.2014.12.011>, 2015.

Drew, D.R., Cannon, D.J., Brayshaw, D.J., Barlow, J.F., and Coker, P.J.: The impact of future offshore wind farms on wind power generation
420 in Great Britain. *Resources*, 4, 1, 155-171, 2015.

El-Asha, S., Zhan, L., and Lungo, G.V.: Quantification of power losses due to wind turbine wake interactions through SCADA meteorological
and wind LiDAR data, *Wind Energy*, 20, 1823-1839, 2017.

Emeis, S.: A simple analytical wind park model considering atmospheric stability. *Wind Energy*, 13, 459-469, 2010.

Emeis, S.: Analysis of some major limitations of analytical top-down wind farm models. *Bound.-Layer Meteorol.*, 187, 423–435, 2022.



425 Emeis, S., Siedersleben, S., Lampert, A., Platis, A., Bange, J., Djath, B., Schulz-Stellenfleth, J., and Neumann, T.: Exploring the wakes of large offshore wind farms. *Journal of Physics: Conference Series* 2016, 753, 092014 (11 pp.) DOI: 10.1088/1742-6596/753/9/092014, 2016.

FINO1: FINO1 – Research Platform in the North and Baltic Seas No. 1, available at: <https://www.fino1.de/en/>, last access: 14 February 2024, 2025.

430 Finserås, E., Herrera Anchustegui, I., Cheynet, E., Gebhardt, C.G., and Reuder, J.: Gone with the Wind? Wind Farm-Induced Wakes and Regulatory Gaps, *Marine Policy*, 159, 105897, <https://doi.org/10.1016/j.marpol.2023.105897>, 2024.

Fitch, A.C., Olson, J.B., Lundquist, J.K., Dudhia, J., Gupta, A.K., Michalakes, J., and Barstad, I.: Local and Mesoscale Impacts of Wind Farms as Parameterized in a Mesoscale NWP Model. – *Mon. Wea. Rev.* 140, 3017–3038, DOI: 10.1175/MWR-D-11-00352.1, 2012.

435 Foreman, R. J., Cañadillas, B., and Robinson, N.: The atmospheric stability dependence of far wakes on the power output of downstream wind farms, *Energies*, 17, 2, 488, <https://doi.org/10.3390/en17020488>, 2024.

Foreman, R.J., Birzer, C., and Cañadillas, B.: Measuring and Simulating Wind Farm Wakes in the North Sea for Use in Assessing Other Regions. *Energies*, 18, 20, 5538, <https://doi.org/10.3390/en18205538>, 2025.

Gebraad, P.M.O., Churchfield, M.J., and Fleming, P.A.: Incorporating Atmospheric Stability Effects into the FLORIS Engineering Model of Wakes in Wind Farms, *J. Phys.: Conf. Ser.*, 753 052004, <https://doi.org/10.1088/1742-6596/753/5/052004>, 2016.

440 Global Wind Energy Council, Global Offshore Wind Report, HY1, <https://tethys.pnnl.gov/sites/default/files/publications/Williams-et-al-2025.pdf>, accessed on 7 November 2025, 2025.

Hersbach, H and Stoffelen, A and De Haan, S: An improved C-band scatterometer ocean geophysical model function: CMOD5, *Journal of Geophysical Research: Oceans*, 112, C3, 10.1029/2006JC003743, 2007.

Ladenburg, J.: Visual impact assessment of offshore wind farms and prior experience, *Appl. Energy*, 86, 3, 380-387, 2009.

445 Lanzilao, L., and Meyers J.: A parametric large-eddy simulation study of wind-farm blockage and gravity waves in conventionally neutral boundary layers, *Journal of Fluid Mechanics*, 979, A54. doi:10.1017/jfm.2023.1088, 2024.

Lampert, A., Bärfuss, K., Platis, A., Siedersleben, S., Djath, B., Cañadillas, B., Hankers, R., Bitter, M., Feuerle, T., Schullz, H., Rausch, T., Angermann, M., Schwitthal, A., Bange, J., Schulz-Stellenfleth, J., Neumann, T., and Emeis, S.: In-situ airborne measurements of atmospheric and sea surface parameters related to offshore wind parks in the German Bight, *Earth Syst. Sci. Data*, 12, 935–946, 2020.

450 Lampert, A., Hankers, R., Feuerle, T., Rausch, T., Cremer, M., Angermann, M., Bitter, M., Füllgraf, J., Schulz, H., Bestmann, U., and Bärfuss, K. B.: In situ airborne measurements of atmospheric parameters and airborne sea surface properties related to offshore wind parks in the German Bight during the project X-Wakes, *Earth Syst. Sci. Data*, 16, 4777–4792, <https://doi.org/10.5194/essd-16-4777-2024>, 2024.

Lange, B., Larsen, S., Höjstrup, J., and Barthelmie, R.: Importance of thermal effects and sea surface roughness for offshore wind resource assessment, *J. Wind Engineering and Industrial Aerodynamics*, 92, 959-988, 2004.

455 Larsen, X.G. and Fischereit, J.: A case study of wind farm effects using two wake parameterizations in the Weather Research and Forecasting (WRF) model (V3.7.1) in the presence of low-level jets, *Geosci. Model Dev.*, 14, 3141–3158, 2021.

Larsén, X.G., Fischereit, J., Hamzeloo, S., Bärfuss, K., and Lampert, A.: Investigation of wind farm impacts on surface waves using coupled numerical simulations, *Renewable Energy*, 237, 121671, <https://doi.org/10.1016/j.renene.2024.121671>, 2024.

Lee, S., Churchfield, M.J., Moriarty, P.J., Jonkman, J., and Michalakes, J.: A Numerical Study of Atmospheric and Wake Turbulence Impacts 460 on Wind Turbine Fatigue Loadings, *J. Solar energy Engineering*, 135, 031001, 10 p., 2013.

Lenschow, D. H.: The Measurement of Air Velocity and Temperature Using the NCAR Buffalo Aircraft Measuring System; National Center for Atmospheric Research, Boulder, CO, NCARTN/EDD-74, 39 pp., <https://doi.org/10.5065/D6C8277W>, 1972.



Li, X., and Lehner, S.: Observation of TerraSAR-X for studies on offshore wind turbine wake in near and far fields, *IEEE J Sel Top Appl Earth Observ Remote Sens.*, 6, 3, 1757-1768, 2013.

465 Lian, Z., Liu, K., and Yang, T.: Potential Influence of Offshore Wind Farms on the Marine Stratification in the Waters Adjacent to China, *J. Mar. Sci. Eng.*, 10, 1872, <https://doi.org/10.3390/jmse10121872>, 2022.

Lundquist, J., DuVivier, K.K., Kaffine, D., and Tomaszewski, J.M.: Costs and consequences of wind turbine wake effects arising from uncoordinated wind energy development, *Nature Energy*, 4, 26-34, 2019.

470 Manzano-Agugliaro, F., Sanchez-Calero, M., Alcayde, A., San-Antonio-Gomez, C., Pereo-Moreno, A.-J., and Salmeron-Manzano, E.: Wind Turbine Offshore Foundations and Connections to Grid, *Inventions* 2020, 5, 1, 8, 2020.

Meijer, J., Steinfeld, G., Vollmer, L., and Dörenkämper, M.: The global blockage effect of a wind farm cluster - an LES study, *J. Phys.: Conf. Ser.*, 2767, 092093, DOI 10.1088/1742-6596/2767/9/092093, 2024.

Mora, E.B., Spelling, J., van der Weijde, A.H., Pavageau, E.-M.: The effects of mean wind speed uncertainty on project finance debt sizing for offshore wind farms, *Applied Energy*, 252, 113419, <https://doi.org/10.1016/j.apenergy.2019.113419>, 2019.

475 Nygaard, N.G., and Hansen, S.D.: Wake effects between two neighbouring wind farms, *Journal of Physics: Conference Series*, 753, 3, 032020, 2016.

Nygaard, N.G., Steen, S.T., Poulsen, L., and Pedersen, J.G.: Modelling cluster wakes and wind farm blockage, *J. Phys.: Conf. Ser.*, 1618, 062072, <https://doi.org/10.1088/1742-6596/1618/6/062072>, 2020.

Olsen, A.-M., Øiestad, M., Berge, E., Køltzow, M.Ø, and Valkonen, T.: Evaluation of Marine Wind Profiles in the North Sea and Norwegian Sea Based on Measurements and Satellite-Derived Wind Products, *Tellus A: Dynamic Meteorology and Oceanography*, 74, 1-16, 480 <https://doi.org/10.16993/tellusa.43>, 2022.

Ouro, P., Ghobrial, M., Ali, K., and Stallard, T.: Numerical modelling of offshore wind-farm cluster wakes, *Renewable and Sustainable Energy Reviews*, 115526, 215, <https://doi.org/10.1016/j.rser.2025.115526>, 2025.

Pedersen, J.G., Svensson, E., Poulsen, L., and Nygaard, N.G.: Turbulence Optimized Park model with Gaussian wake profile, *J. Phys.: Conf. Ser.*, 2265, 022063, <https://doi.org/10.1088/1742-6596/2265/2/022063>, 2022.

Pedersen, M.M., Meyer Forsting, A., van der Laan, P., Riva, R., Alcayaga Romàn, L.A., Criado Risco, J., Friis-Møller, M., Quick, J., Schøler Christiansen, J.P., Valotta Rodrigues, R., Olsen, B.T., and Réthoré, P.-E.: PyWake 2.5.0: An open-source wind farm simulation tool, DTU Wind, Technical University of Denmark, February 2023.

490 Peña, A., Gryning, S.-E., and Floors, R.: Lidar observations of marine boundary-layer winds and heights: a preliminary study, *Meteorologische Zeitschrift*, 24, 6, 581-589, 2015.

Pettas, V., Kretschmer, M., Clifton, A., and Cheng, P.W.: On the effects of inter-farm interactions at the offshore wind farm Alpha Ventus, *Wind Energ. Sci.*, 6, 1455-1472, 2021.

Paskyabi, M.B.: Offshore Wind Farm Wake Effect on Stratification and Coastal Upwelling, *Energy Procedia*, 80, 131-140, 2015.

Platis, A., Siedersleben, S., Bange, J., Lampert, A., Bärfuss, K., Hankers, R., Cañadillas, B., Foreman, R., Schulz-Stellenfleth, J., Djath, 495 B., Neumann, T., and Emeis, S.: First in situ evidence of wakes in the far field behind offshore wind farms, *Scientific Reports*, doi 10.1038/s41598-018-20389-y, 2018.

Platis, A., Bange, J., Bärfuss, K., Cañadillas, B., Hundhausen, M., Djath, B., Lampert, A., Schulz-Stellenfleth, J., Siedersleben, S., Neumann, T., and Emeis, S.: Long-range modifications of the wind field by offshore wind parks – results of the project WIPAFF, *Meteorologische Zeitschrift*, DOI: 10.1127/metz/2020/1023, 22 pp., 2020.



500 Platis, A., Hundhausen, M., Lampert, A., Emeis, S., and Bange, J.: The Role of Atmospheric Stability and Turbulence in Offshore Wind-Farm Wakes in the German Bight, *Boundary-Layer Meteorology*, <https://doi.org/10.1007/s10546-021-00668-4>, 29 pp., 2021a.

Platis, A., Hundhausen, M., Mauz, M., Siedersleben, S., Lampert, A., Bärfuss, K., Djath, B., Schulz-Stellenfleth, J., Cañadillas, B., Neumann, T., Emeis, S., and Bange, J.: Evaluation of a simple analytical model for offshore wind farm wake recovery by in situ data and Weather Research and Forecasting simulations, *Wind Energy*, 24, 212–228, 2021b.

505 Platis, A., Büchau, Y., Zuluaga, S., and Bange, J.: The impact of offshore wind farms on the latent heat flux, *Boundary-Layer Meteorology*, 32, 4, 261-277, https://www.schweizerbart.de/papers/metz/detail/32/102963/The_impact_of_offshore_wind_farms_on_the_latent_he?af=crossref, 2023.

Ponce de León, S., Bettencourt, J.H., and Kjerstad, N.: Simulation of Irregular Waves in an Offshore Wind Farm with a Spectral Wave Model, *Cont. Shelf Res.*, 31, 1541–1557, 2011.

510 Porchetta, S., Munoz-Esparza, D., Munters, W., van Beeck, J., and van Lipzig, N.: Impact of ocean waves on offshore wind farm power production, *Renewable energy*, 180, 1179–1193, <https://doi.org/10.1016/j.renene.2021.08.111>, 2021.

Porté-Agel, F., Bastankhah, M. and Shamsoddin, S.: Wind-Turbine and Wind-Farm Flows: A Review, *Boundary-Layer Meteorol.*, 174, 1–59, <https://doi.org/10.1007/s10546-019-00473-0>, 2020.

Pryor, S.C., and Barthelmie, R.J.: A global assessment of extreme wind speeds for wind energy applications, *Nat. Energy*, 6, 268–276, 515 <https://doi.org/10.1038/s41560-020-00773-7>, 2021.

Rausch, T., Bärfuss, K., Hankers, R., Bitter, M., Feuerle, T., Cremer, M., Angermann, M., Füllgraf, J., and Lampert, A.: In-situ airborne measurements of atmospheric and sea surface parameters related to offshore wind parks in the German Bight [dataset publication series]. PANGAEA, <https://doi.org/10.1594/PANGAEA.955382>, 2023.

Rausch, T., Cañadillas, B., and Lampert, A.: Coastal vertical wind lidar measurements of horizontal wind speed and wind direction from 520 40 to 500 m at Norderney island, German Bight, North Sea, Germany [dataset]. PANGAEA, <https://doi.org/10.1594/PANGAEA.953770>, 2023.

Rivier, S., Bennis, A.-C., Pinon, G., Magar, V., and Gross, M.: Parameterization of wind turbine impacts on hydrodynamics and sediment transport, *Ocean Dynamics*, 66, 1285–1299, 2016.

525 Sanchez Gomez, M., Lundquist, J.K., Mirocha, J.D., and Arthur, R.S.: Investigating the physical mechanisms that modify wind plant blockage in stable boundary layers, *Wind Energ. Sci.*, 8, 1049–1069, <https://doi.org/10.5194/wes-8-1049-2023>, 2023.

Sathe, A., Mann, J., Barlas, T., Bierbooms, W.A.A.M., van Bussel, G.J.W.: Influence of atmospheric stability on wind turbine loads, *Wind Energy*, 16, 1013–1032, doi:10.1002/we.1528, 2013.

Schmidt, J., Vollmer, L., Dörenkämper, M., and Stoevesandt, B.: FOXES: Farm Optimization and eXtended yield Evaluation Software, *Journal of Open Source Software*, 8, 86, 5464, <https://doi.org/10.21105/joss.05464>, 2023.

530 Schmitt, L., Bärfuss, K.B., Larsen, X.G., Fischereit, J., and Lampert, A.: Spatial Variability of Sea State in the German Bight and Influence of Offshore Wind Farms, submitted to *Wind Energy*, 2025.

Schneemann, J., Rott, A., Dörenkämper, M., Steinfeld, G., and Kühn, M.: Cluster wakes impact on a far-distant offshore wind farm's power, *Wind Energ. Sci.*, 5, 29–49, 2020.

Schneemann, J., Theuer, F., Rott, A., Dörenkämper, M., and Kühn, M.: Offshore wind farm global blockage measured with scanning lidar, 535 *Wind Energ. Sci.*, 6, 521–538, <https://doi.org/10.5194/wes-6-521-2021>, 2021.

Schneemann, J., Theuer, F., Rott, A., and Kühn, M.: Measurement of flow deflection effects around an offshore wind farm caused by global blockage, *J. Phys.: Conf. Ser.*, 3016, 012012, DOI 10.1088/1742-6596/3016/1/012012, 2025.



540 Schulz-Stellenfleth, J., Emeis, S., Dörenkämper, M., Bange, J., Cañadillas, B., Neumann, T., Schneemann, J., Weber, I., zum Berge, K., Platis, A., Djath, B., Gottschall, J., Vollmer, L., Rausch, T., Barekzai, M., Hammel, J., Steinfeld, G., and Lampert, A.: Coastal impact on offshore wind farms – a review focusing on the German Bight area, *Meteorologische Zeitschrift*, 31, 4, 289 - 315, 2022.

545 Sengers, B.A.M., Vollmer, L., and Dörenkämper, M.: Multi-model approach for wind resource assessment, *J. Phys.: Conf. Ser.*, 2767, 092024, <https://doi.org/10.1088/1742-6596/2767/9/092024>, 2024.

550 Shaw, W. J., Berg, L. K., Debnath, M., Deskos, G., Draxl, C., Ghate, V. P., Hasager, C. B., Kotamarthi, R., Mirocha, J. D., Muradyan, P., Pringle, W. J., Turner, D. D., and Wilczak, J. M.: Scientific challenges to characterizing the wind resource in the marine atmospheric boundary layer, *Wind Energ. Sci.*, 7, 2307–2334, <https://doi.org/10.5194/wes-7-2307-2022>, 2022.

555 Siedersleben, S.K., Platis, A., Lundquist, J.K., Lampert, A., Bärfuss, K., Cañadillas, B., Djath, B., Schulz-Stellenfleth, J., Neumann, T., Bange, J., and Emeis, S.: Evaluation of a Wind Farm Parametrization for Mesoscale Atmospheric Flow Models with Aircraft Measurements, *Meteorologische Zeitschrift*, PrePub DOI 10.1127/metz/2018/0900, 2018a.

560 Siedersleben, S.K., Lundquist, J.K., Platis, A., Bange, J., Bärfuss, K., Lampert, A., Cañadillas, B., Schulz-Stellenfleth, J., Bange, J., Neumann, T., and Emeis, S.: Micrometeorological impacts of offshore wind farm as seen in observations and simulations, *Env. Res. Lett.*, 13, 124012, 2018b.

565 Siedersleben, S., Platis, A., Lundquist, J.Djath, B., Lampert, A., Bärfuss, K., Cañadillas, B., Schulz-Stellenfleth, J., Bange, J., Neumann, T., and Emeis, S.: Turbulent kinetic energy over large offshore wind farms observed and simulated by the mesoscale model WRF (3.8.1), *Geosci. Model Dev.*, 13, 249–268, 2020.

570 Skamarock, W. C., Klemp, J. B., Dudhia, J., Gill, D. O., Liu, Z., Berner, J., Wang, W., Powers, J. G., Duda, M. G., Barker, D., and Huang, X.-Y.: A Description of the Advanced Research WRF Version 3, NCAR Technical Note NCAR/TN-556+STR, National Center for Atmospheric Research, Boulder, Colorado, USA, 162 pp., <https://doi.org/10.5065/1dfh-6p97>, 2019.

575 Spangehl, T., Borsche, M., Niermann, D., Kaspar, F., Schimanke, S., Brienen, S., Möller, T., and Brast, M.: Intercomparing the quality of recent reanalyses for offshore wind farm planning in Germany's exclusive economic zone of the North Sea, *Adv. Sci. Res.*, 20, 109–128, <https://doi.org/10.5194/asr-20-109-2023>, 2023.

580 Spyridonidou, S., and Vagiona, D.G.: Systematic Review of Site-Selection Processes in Onshore and Offshore Wind Energy Research, *Energies* 13, 5906, 2020.

585 Stickney, T. M., Shedlov, M. W., and Thompson, D. I.: Goodrich Total Temperature Sensors, Technical Report, 5755, 32 pp. available at: <https://www.flighthdatacommunity.com/wp-content/uploads/downloads/2013/02/TAT-Report.pdf> (accessed on 18 April 2022), 1994.

590 van Stratum, B., Theeuwes, N., Barkmeijer, J., van Ulft, B., and Wijnant, I.: A one-year-long evaluation of a wind-farm parameterization in HARMONIE-AROME. *Journal of Advances in Modeling Earth Systems*, 14, e2021MS002947. <https://doi.org/10.1029/2021MS002947>, 2022.

595 Taylor, P.A.: A model of airflow above changes in surface heat flux, temperature and roughness for neutral and unstable conditions, *Boundary-Layer Meteorology*, 1, 18-39, DOI:10.1007/BF00193902, 1970.

600 UL-International, Openwind User Manual, Version 1.9, AWS Truepower, LLC, Albany, NY, USA, 2020.

605 Veers, P., Dykes, K., Lantz, E., Barth, S., Bottasso, S.B., Carlson, O., Clifton, A., Green, J., Holttinen, H., Laird, D., Lehtomäki, V., Lundquist, J.K., Manwell, J., Marquis, M., Meneveau, C., Moriarty, P., Munduate, X., Muskulus, M., Naughton, J., Pao, L., Paquette, J., Peinke, J., Robertson, A., Sanz Rodrigo, J., Sempreviva, A.M., Smith, J.C., Tuohy, A., and Wiser, R.: Grand challenges in the science of wind energy, *Science*, 366, 443, 2019.

610 Vera-Tudela, L., and Kühn, M.: Analysing wind turbine fatigue load prediction: The impact of wind farm flow conditions, *Renew. Energ.*, 107, 352-360, 2017.



Verhoef, A., Portabella, M., Stoffelen, A., and Hersbach, H. (2008). CMOD5. n-the CMOD5 GMF for neutral winds. Tech. Rep. SAF/OSI/C-DOP/KNMI/TEC/TN/3, 165, KNMI, De Bilt, Netherlands, 2017.

Vollmer, L., Sengers, B. A. M., and Dörenkämper, M.: Brief communication: A simple axial induction modification to the Weather Research and Forecasting Fitch wind farm parameterization, *Wind Energ. Sci.*, 9, 1689–1693, <https://doi.org/10.5194/wes-9-1689-2024>, 2024.

580 580 Wagner, D. Steinfeld, G., Witha, B., Wurps, H., and Reuder, J.: Low Level Jets over the Southern North Sea, *Meteorologische Zeitschrift*, 28, 5, 389 - 415, DOI: 10.1127/metz/2019/0948, 2019.

Windt, C., Goseberg, N., Schimmels, S., Kudella, M., Shanmugasundaram, R., Rusche, H., Vanjakula, V., Adam, F., Majewski, M., Kazimierowicz-Frankowska, K., Pietrzkiewicz, M., Kirca, V.S.O., Sumer, B.M.: Liquefaction around marine structures: Development of a numerical modelling framework in OpenFOAM, *Int. J. Offshore Polar Engineering*, 34, 2, 2024.

585 585 Wiser, R., Rand, J., Seel, J., Beiter, P., Baker, E., Lantz, E., and Gilman, P.: Expert elicitation survey predicts 37% to 49% declines in wind energy costs by 2050, *Nature Energy*, 6, 5555-565, 2021.

Wu, Y.T., and Porté-Agel, F.: Large-Eddy Simulation of Wind-Turbine Wakes: Evaluation of Turbine Parametrisations, *Boundary-Layer Meteorol.*, 138, 345–366, <https://doi.org/10.1007/s10546-010-9569-x>, 2011.